



Published in final edited form as:

*Cancer Gene Ther.* 2016 July ; 23(7): 221–228. doi:10.1038/cgt.2016.21.

## Trastuzumab-targeted gene delivery to Her2-overexpressing breast cancer cells

Kristine Mann, Ph.D.<sup>1,2,\*</sup> and Max Kullberg, Ph.D.<sup>2,\*</sup>

<sup>1</sup>Department of Biological Sciences, University of Alaska Anchorage, Anchorage, AK 99508, USA

<sup>2</sup>WWAMI Medical Education Program, University of Alaska Anchorage, Anchorage, AK 99508, USA

### Abstract

We describe a novel gene delivery system that specifically targets Her2-overexpressing breast cancer cells. The targeting complexes consist of a PEGylated polylysine core that is bound to DNA molecules coding for either green fluorescent protein or shrimp luciferase. The complex is disulfide linked to the monoclonal antibody trastuzumab and to a pore-forming protein, Listeriolysin O (LLO). Trastuzumab is responsible for specific targeting of Her2 receptors and uptake of the gene delivery complex into endosomes of recipient cells, while LLO ensures that the DNA molecules are capable of transit from the endosomes into the cytoplasm. Omission of either trastuzumab or LLO from the nanocomplexes results in minimal gene product in targeted cells. Treatment of isogenic MCF7 and MCF7/Her18 cell lines, differing only in number of Her2 receptors, with the complete gene delivery system results in a 30-fold greater expression of luciferase activity in the Her2-overexpressing MCF7/Her18 cells. Our nanocomplexes are small (150-250 nm), stable to storage, non-toxic, and generic in make-up such that any plasmid DNA or antibody specific for cell-surface receptors can be coupled to the PEGylated polylysine core.

### Introduction

The goal of cancer gene therapy is to deliver therapeutic genes and achieve their expression in tumor tissue. Candidate genes include IL-12, which could provoke an anti-tumor immune response, and TNF-alpha which could induce cancer cell apoptosis. However, these genes must be delivered specifically to avoid toxic side effects. Targeted delivery of genes to cancer cells has been achieved in a limited number of laboratories using liposomal delivery systems with antibody to Her2 receptors (1,2), with an RGD peptide specific for integrin (3), or with antibody to prostate-specific membrane antigen (4).

Alternative gene delivery systems have been based on polymers such as polyethylenimines (PEI) or dendrimers, rather than on liposomes. Such polymeric targeting systems have been

---

Users may view, print, copy, and download text and data-mine the content in such documents, for the purposes of academic research, subject always to the full Conditions of use: [http://www.nature.com/authors/editorial\\_policies/license.html#terms](http://www.nature.com/authors/editorial_policies/license.html#terms)

\*To whom correspondence should be addressed. Tel: 01-907-786-1615; Fax: 01-907-786-4700; [kmann1@uaa.alaska.edu](mailto:kmann1@uaa.alaska.edu) or [mpkullberg@uaa.alaska.edu](mailto:mpkullberg@uaa.alaska.edu).

**Conflict of Interest:** The authors declare no conflict of interest.

reported using epidermal growth factor (EGF) specific for EGF receptors (5), anti-Her2 antibody (trastuzumab) specific for Her2 receptors (6), transferrin specific for transferrin receptors (7,8), a fibroblast growth factor (FGF)-11-mer peptide specific for FGF receptors (9), and lactoferrin or lactoferricin specific for transferrin receptors (10).

There are, however, problems associated with the use of polymeric-based targeting systems. PEI is highly cytotoxic, causing immediate disruption of the cell membrane and consequent necrotic cell death, or eventual disruption of the mitochondrial membrane leading to apoptosis (11). Toxicity has been decreased somewhat by using lower molecular weight PEIs (12) or by shielding of PEI/DNA complexes via covalent modification with polyethylene glycol (PEG) to prevent non-specific interactions with components in the plasma or with erythrocytes (12).

In contrast to gene targeting systems based on liposomes or on PEI- or dendrimer- polymers, the targeting complex we have developed is based on polylysine (PL), a non-toxic polymer, coupled to a N-hydroxysuccinimide and orthopyridyl disulfide hetero-functionalized PEG ester (OPSS-PEG-NHS). By including bound trastuzumab (Herceptin®), our targeting complexes selectively deliver reporter DNAs to breast cancer cells overexpressing Her2 receptors. The test reporter genes used in our system code for either green fluorescent protein (GFP) or luciferase (Luc). Expression of these DNAs is dependent on the inclusion of a pore-forming protein, Listeriolysin O (LLO), in the targeting complexes, to enable passage of the DNAs from the endosomal compartment to the interior of the targeted cells.

The practical advantage of these complexes is that they are generic in nature and are designed to carry any antibody recognizing a specific membrane receptor overexpressed in the targeted tumor cells and likewise to carry any DNA molecule coding for a specific gene product in the targeted cells. Our nanocomplexes result in gene expression in specifically targeted cells and appear to be non-toxic to the recipient cells.

## Materials and Methods

### Materials

Orthopyridyl disulfide functionalized polyethylene glycol N-hydroxysuccinimide ester (OPSS-PEG-NHS, MW 5000) was purchased from Nanocs, Inc. (New York, NY). Trastuzumab (Herceptin®) was a generous gift from Dr. Virginia Borges (UC Denver, CO, USA). Listeriolysin O (LLO) from *E. coli* transfected with the LLO-pEt29-DP-E3570 plasmid, kindly provided by Dr. Dan Portnoy (UC Berkeley, CA, USA), was purified by the method described previously (13,14) and stored in storage buffer (50 mM phosphate buffer, pH 6.0, 1 M NaCl, 1 mM EDTA) without dithiothreitol (DTT) to preserve its activity. Polylysine hydrobromide (MW 37,000; degree of polymerization: 177) and 2-iminothiolane-HCl (Traut's reagent) were purchased from Sigma Life Science (St. Louis, MO, USA). CL-4B Sepharose used for the purification of the one-component complexes was purchased from Amersham Biosciences (Uppsala, Sweden). All other reagents, unless otherwise specified, were purchased from Thermo Fisher Scientific (Pittsburgh, PA, USA).

## Cells and growth medium

The cell line ce2, derived from human mammary epithelial cell line MTSV1-7 that had been stably transfected with Her2 DNA (15), was kindly provided by Dr. Joyce Taylor-Papadimitriou (King's College, London School of Medicine, London, UK). The overexpressing-Her2 ce2 cells were grown in Dulbecco's modified Eagle's medium (DMEM, Sigma Life Science) with 10% fetal bovine serum (Irvine Scientific, Irvine, CA, USA), supplemented with 1  $\mu$ M insulin and 5  $\mu$ M dexamethasone. Isogenic cell lines MCF7 and MCF7/Her18 were kindly provided by Dr. Hung Mien-Chie (M.D. Anderson Cancer Center, Houston, TX, USA) and were grown in DMEM/nutrient mixture F-12 Ham (Sigma Life Science) containing 10% fetal bovine serum and 1% penicillin-streptomycin. The MCF7/Her18 cell line (referred to as Her18 in this report) overexpresses the Her2 cell surface receptor by 45-fold as a result of stable transfection of the MCF7 cell line with Her2 DNA (16). The HCC1954 cell line, derived from an invasive ductal carcinoma, was purchased from ATCC (Manassas, VA) and grown in RPMI 1640 medium (Corning Mediatech, Manassas, VA) with 10% fetal bovine serum (Gibco).

## DNAs and purification

DH5 $\alpha$  bacteria transfected with the pEGFP-N3 plasmid were kindly provided by Dr. Jason Burkhead (University of Alaska, Anchorage, AK, USA). After growth of the bacteria in LB broth with kanamycin at a final concentration of 30  $\mu$ g/ml, endotoxin-free DNA coding for the jellyfish green fluorescent protein (GFP) was prepared using the Macherey-Nagel (Bethlehem, PA, USA) NucleoBond Xtra midi EF kit. Shrimp luciferase plasmid DNA (5.9 kb) with a CMV promoter, also known as NanoLuc, was a generous gift from Promega (Madison, WI), and was used to transfect *E. coli*. After growth of the transfected bacteria in LB broth with ampicillin at a final concentration of 50  $\mu$ g/ml, endotoxin-free shrimp luciferase DNA was prepared using the same Macherey-Nagel EF kit specified above.

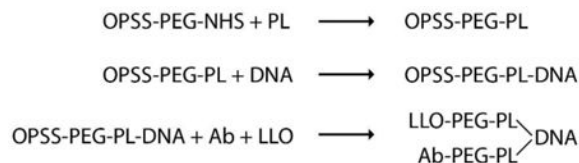
## Nanocomplex preparation and characterization

The nanocomplexes were prepared in a series of steps as follows. OPSS-PEG-NHS (referred to as OPN) was made up as a stock solution of 1 mg OPN/ml chloroform and stored at -20°C. For a nanocomplex preparation, 100  $\mu$ l of OPN was taken and dried down for 1 hr under nitrogen at 45°C. It was subsequently rehydrated with 200  $\mu$ l of polylysine (PL) stock solution at a concentration of 0.5 mg/ml H<sub>2</sub>O by pipetting vigorously at 37°C for 2 mins. After being left at 37°C for another 15 mins, the OPN/PL (ratio of 100  $\mu$ g OPN / 100  $\mu$ g PL) mixture was put at 4°C overnight to complete the formation of covalent amide bonds between the lysines and the NHS-groups on the OPN.

DNA (either pEGFP-N3 or shrimp luciferase plasmid) from a stock solution at a concentration of 1 mg DNA/ml H<sub>2</sub>O was added slowly with mixing to the requisite volume of OPN/PL (now referred to as OPPL) and left at room temperature for 4-5 hrs. The molar weight ratio of OPPL to DNA was 2:1, to give an approximate cationic charge ratio of 4:1. At the end of the binding period, 1/10 $\times$  volume of 10 $\times$  Dulbecco's phosphate-buffered saline (DPBS), pH 6.9, was added slowly with mixing to the OPPL-DNA, in order to adjust the pH to 7.4-7.5 for the subsequent reactions with LLO and with thiolated trastuzumab.

For the purposes of binding trastuzumab (Tmab) to the OPSS groups in OPPL-DNA, thiol groups were introduced into the trastuzumab molecules. The thiolated trastuzumab (t-Tmab) was prepared just before addition to the OPPL-DNA as follows. A given volume (equal to 0.8 mg) of trastuzumab (stock solution at 20 mg/ml) was diluted with an equal volume of H<sub>2</sub>O, 1/10× volume of 10× DPBS, pH 6.9, and 1/100× volume of 0.5M EDTA, and then 17 μg Traut's reagent in 1× DPBS, pH 7.45 was added and mixed to give a molar ratio of Traut's : trastuzumab of 20:1. The thiolation reaction proceeded for 1 hr at room temperature and was then stopped by loading onto a Zeba desalting column (7K MWCO from ThermoScientific) which had been prewashed 4× with 1× DPBS, pH 7.45. The t-Tmab was recovered by spinning the column in an Eppendorf microfuge model 5417R at 1450 × g for 2 mins at 4°C, to remove the unreacted Traut's reagent.

A 10 μl aliquot of 1× DPBS, pH 7.45 was added to 1/2× final volume (~130 μl) of OPPL-DNA, followed by mixing in 3 μl purified LLO (~6 μg or  $1 \times 10^{-4}$  moles) and 1/4× (~0.2 mg) volume of t-Tmab recovered from the desalting column. The competitive reaction of LLO and t-Tmab for binding to the OPSS group in the OPPL-DNA was allowed to proceed 16-18 hrs overnight at room temperature. When either LLO or t-Tmab was omitted from the reaction, an equivalent volume of corresponding buffer was added instead. The steps in preparation of the targeting complexes are summarized below:



The following day, a RBC lysis assay was carried out to determine if LLO had completely reacted with the OPPL-DNA to yield the Tmab/DNA complex. A 5 μl aliquot of the reaction mixture was placed in each of two tubes, with 2.5 μl 300 mM DTT added to one tube and 2.5 μl H<sub>2</sub>O added to the other tube, mixed and incubated at room temperature for 15 mins to allow for reduction of the disulfide bond. Sheep red blood cells were prepared by centrifugation and resuspension of the pellet in 1× DPBS, pH 7.45 at a 1 in 2.5 dilution. At the end of the 15-minute incubation, 50 μl of the diluted red blood cells (RBCs) were added to each of the two tubes and the time until lysis was noted. If LLO had fully reacted with the OPSS group, there was no lysis of the RBCs in the presence of water, whereas in the presence of DTT there was complete lysis of the RBCs within 2-3 minutes.

If the reaction of LLO with the Tmab/DNA complex had gone to completion, the reaction mixture was put over a CL-4B column pre-equilibrated with 1× DPBS, pH 7.45, and fractions were collected. To identify the early-eluting DNA-nanocomplex fractions, aliquots of the fractions were placed in a mini-spectrophotometer (Eppendorf BioPhotometer) and A260, A280, and A320 readings of each fraction were recorded. The peak nanocomplex fractions, characterized by a peak in absorption at all 3 wavelengths, were stored at 4°C until use in the cell treatment experiments.

Sizing of the nanocomplex preparations was determined by dynamic light scattering analysis using a Nicomp 380 zeta potential/particle sizer (Particle Sizing Systems, Santa Barbara,

CA) or using a Malvern zetasizer Nano-S (Malvern Instruments Ltd., Malvern, UK). When the effect of presence versus absence of trastuzumab on DNA expression was tested, the size of the complete complex with both t-Tmab and LLO was  $278 \pm 94$  nm while that of the complex with LLO but minus t-Tmab was  $267 \pm 107$  nm. When the effect of LLO was tested on DNA expression, the size of the complete complex with both t-Tmab and LLO was  $147 \pm 31$  nm, while that of the complex with Tmab but minus LLO was  $148 \pm 37$  nm. For unknown reasons, some variability in the size of the nanocomplex preparations was noted, although within a given experiment the relative sizes of the complexes were well matched. In general, it can be seen that the range in nanocomplex size is between 150 and 250 nm approximately.

### Treatment of cells with nanocomplexes

Actively growing ce2, HCC1954, MCF7, and MCF7/Her18 cells were plated out in Falcon microtest 96-well assay plates, black/clear bottom (Becton Dickinson Labware, Franklin Lakes, NJ, USA), either in duplicate for fluorescence analysis or in triplicate for luciferase analysis. After 48 hours of growth, when the cells were between 50%-70% confluent, they were treated with the nanocomplex preparations. Prior to treatment, the CL-4B-purified nanocomplex preparations were equalized with respect to the amount of DNA bound using the Qubit ds DNA high-sensitivity (HS) assay kit (Invitrogen Life Technologies, Thermo Fisher Scientific Inc., Pittsburgh, PA, USA).

Treatment mixes were made up just prior to addition to the cells, with the nanocomplexes being added last to the mixture. After removal of the old growth medium from the cells, the final volume of treatment mix added to each well was 100  $\mu$ l, made up of the appropriate growth medium (75  $\mu$ l – 80  $\mu$ l), 5  $\mu$ l to 20  $\mu$ l of nanocomplex preparation, an equalizing volume of 1 $\times$  DPBS, pH 7.45, and 2.5  $\mu$ l of free Tmab when tested for competition purposes. After 3 hrs of treatment at 37°C in 5% CO<sub>2</sub>, the treatment mix was removed from each well, 100  $\mu$ l of fresh growth medium with 2% penicillin-streptomycin was added to each well, and the cells were grown at 37°C in 5% CO<sub>2</sub> for another 48 hrs before examining GFP fluorescence or for 24 hrs before measuring luciferase activity.

### Analysis of gene expression

For examination of GFP fluorescence, the growth medium was removed from the ce2 cells, and 100  $\mu$ l 1 $\times$  DPBS, pH 7.45 was added to each well. The cells were viewed with a Leica DMI6000B inverted fluorescence microscope, and photos were taken with a 5 $\times$  objective using Leica Application Suite, version 3.7.0 software. For the purposes of quantitation, NIH ImageJ was used to compare the relative amounts of fluorescence in each field of cells subjected to different conditions of treatment with the nanocomplexes.

For measuring luciferase activity, the growth medium was removed from the MCF7 and MCF7/Her18 cells, the cells were rinsed with 100  $\mu$ l 1 $\times$  DPBS, pH7.45, and then 100  $\mu$ l 1 $\times$  reporter lysis buffer (Promega, Madison, WI, USA) was added to each well. Lysis of the cells was enhanced by one freeze-thaw cycle of the 96-well plate at -80°C, followed by transfer of the extracts to microfuge tubes which were spun at 11,900 g for 3 mins at 4°C in an Eppendorf microfuge 5417R. A 5  $\mu$ l aliquot of each extract was diluted with 45  $\mu$ l 1 $\times$

DPBS, pH 7.45, in a white 96-well assay plate and then 50  $\mu$ l of Nano-Glo luciferase assay reagent (Promega) was added to each well. The luminescence produced by each cell extract was measured in a Biotek luminometer using Gen5 software. Protein determinations were done on the same cell extracts using a modification of the BCA protein assay (reagents A and B, Pierce, Rockford, IL, USA) for a 96-well plate (Corning #25860). To each well, we added 100  $\mu$ l BCA reagent (50 parts reagent A : 1 part reagent B) plus 10  $\mu$ l of each cell extract or 10  $\mu$ l of each BSA standard. The wells were mixed, covered with parafilm, heated at 60°C in a dry incubator for 15 mins to develop the color, and then read at 562 nm after removing the parafilm.

### Analysis of nanocomplex toxicity

To analyze if the nanocomplex treatment of cells had any effect on cell viability or proliferation, the XTT cell proliferation assay kit (ATCC, Manassas, VA) was used. Equal numbers of MCF7/Her18 cells were plated out in the requisite number of wells in a 96-well plate at a concentration of  $0.9 \times 10^4$  cells/well and grown overnight at 37°C in a CO<sub>2</sub> incubator. The following day, replicate wells were treated either with 100  $\mu$ l of growth medium (plus 10% fetal bovine serum and penicillin-streptomycin) containing 10  $\mu$ l of luciferase nanocomplex (complex-treated) or with 100  $\mu$ l of medium containing 10  $\mu$ l of 1 $\times$  DPBS, pH 7.45 (control-treated) for 3 hours at 37°C in 5% CO<sub>2</sub>. At the end of a 3-hour incubation, the treatment mix was pipetted off from each well, replaced with 100  $\mu$ l of fresh growth medium, and the treated cells were then grown for another 24, 48, or 72 hours before adding 50  $\mu$ l activated-XTT solution to each well for a further incubation of 3 hours at 37°C. The specific absorbance of the treated (complex- versus control-treated) cells in each well and in the blank medium-only wells was measured at 475nm, followed by measurement of the non-specific absorbance at 660nm. The specific absorbance of each sample was expressed mathematically according to the manufacturer's instructions, as follows:

$$\text{Specific Absorbance (S.A.)} = A_{475\text{nm}} (\text{Test}) - A_{475\text{nm}} (\text{Blank}) - A_{660\text{nm}} (\text{Test})$$

Parallel wells of complex-treated versus control-treated MCF7/Her18 cells were harvested simultaneously at 24, 48, and 72 hours for analysis of luciferase expression, as specified above under 'Analysis of gene expression'.

### Nomenclature

For clarity, our targeting nanocomplexes are named according to their variable components, the targeting antibody and the DNA content. Unless otherwise stated, all constructed complexes contain LLO. All Tmab-complexes bear trastuzumab, whereas non-Tmab-complexes bear no targeting antibody. Tmab/GFP complexes contain GFP DNA; Tmab/Luc complexes contain luciferase DNA.



## Results

### Fluorescence of ce2 cells targeted with Tmab/GFP nanocomplexes

Nanocomplexes specific for Her2 receptors consist of trastuzumab (Tmab) and Listeriolysin O (LLO) conjugated to a PEGylated-polylysine/DNA core. Tmab allows for the specific targeting of Her2-overexpressing cells, while reversibly disulfide-bound LLO facilitates delivery of DNA through the endosome via LLO-formed pores (14,17,18).

Our initial experiments on gene targeting were done with ce2 cells, derived from a human mammary epithelial cell line transfected with Her2-DNA and known to overexpress Her2 receptors (15). Previous work in our laboratory had shown that both Tmab (19) and LLO (14) were essential for specific targeting and delivery of a payload (calcein) to the cytoplasm of these cells. Because of these data, we reasoned that ce2 cells would be a good choice for studying the targeting ability of our GFP-complexes bearing Tmab and LLO.

When ce2 cells were treated with Tmab/GFP nanocomplexes, GFP signal was detectable by 24 hours and increased through 48 hours. We chose the latter time point for our studies on the specificity of delivery. As the treatment dosage of Tmab/GFP targeting complexes was increased from 5  $\mu$ l to 20  $\mu$ l, ce2 cells showed an increase in GFP expression at 48 hours after treatment (Figure 1). We noted a marked decrease in GFP expression both when Tmab was omitted from the targeting complexes and when Tmab/GFP targeting complexes were competed by free Tmab during treatment of the cells (Figure 1). The profile of GFP expression when the complexes were competed with free Tmab was in fact similar to that seen when the targeting antibody was omitted from the nanocomplex preparation (Figures 1 and 2). ImageJ analysis to quantitate the fluorescence showed that the expression level of GFP in the presence of free Tmab as competitor was approximately 20% of that seen when competing free Tmab was not present (Figure 2).

Likewise, GFP expression in ce2 cells was used to evaluate the effect of LLO on targeted gene delivery. The expression of GFP from delivery complexes constructed without LLO was only 5% of the expression from complexes with LLO (Figure 2). Interestingly, this 5% residual expression was further reduced by free Tmab competition, to about 1% of the expression achieved by complexes containing LLO (Figure 3). This result suggests that at least a portion of the GFP expression without LLO is due to Her2 specific uptake of the targeting complexes and leakage of GFP DNA out of the endosome in some other manner than through LLO-formed pores.

### Fluorescence in MCF7/Her18 cells targeted with Tmab/GFP nanocomplexes and competition with free trastuzumab

To visualize the efficiency of DNA delivery to targeted cells, we treated Her2-overexpressing MCF7/Her18 (referred to as Her18) cells with Tmab/GFP complexes and compared bright field images with fluorescence images of cells in the same microscopic field (Figure 4). In this example, a manual count of all visible cells in the bright field and fluorescent images using ImageJ indicated that 18% of the cells expressed detectable GFP (Figure 4, left-hand panels). It can be seen that the level of fluorescence varied from cell to cell within the treated population. Variation in degree of GFP expression in targeted cells

could result from variation in a number of different factors, such as variation in binding of complexes to receptors in the 3-hour incubation period, successful uptake into endosomes, efficiency of transit out of the endosomes, and timing of subsequent transcription and translation.

We also demonstrated that GFP expression was significantly reduced when cells were co-incubated with targeting complexes and free Tmab added at the time of treatment. The reduced expression is presumably due to competitive inhibition by free Tmab on Tmab/GFP complex binding to Her2 receptors (Figure 4, right-hand panels).

### **Effect of Her2 receptor overexpression and requirement of Tmab for targeted delivery of luciferase DNA**

To evaluate the components essential to our nanocomplex delivery system, we compared the expression of targeted DNA in the isogenic breast cancer cell lines MCF7 and MCF7/Her18. The Her18 cell line differs from the parent MCF7 cell line by virtue of a 45-fold increase in the number of Her2 receptors located in its plasma membranes (16). To test the versatility of our nanocomplex system and to simplify the quantitation of the gene product, we replaced the GFP DNA with shrimp luciferase DNA in the targeting complex preparation (Tmab/Luc complexes).

When both the MCF7 and Her18 cell lines were treated with varying doses of Tmab/Luc complexes, there was a 25- to 30-fold increase in the luciferase activity of Her18 cells as compared to that of MCF7 cells (Figure 5). When Tmab was omitted from the complexes (non-Tmab/Luc) used for treatment of the Her18 cells, the luciferase activity was reduced by more than 90% (Figure 5), demonstrating that the specificity for Her18 cells is indeed based on Tmab binding to overexpressed Her2 receptors.

### **Requirement of LLO for expression of luciferase DNA in cells targeted with Tmab/Luc nanocomplexes**

Studies done with Tmab/Luc complexes constructed with or without LLO present in the complex showed that LLO was essential for expression of the luciferase DNA in both Her18 and MCF7 cells (Figure 6). When LLO was present, 20- to 22-fold more luciferase activity was expressed in the Her18 cells than in the MCF7 cells (Figure 6). It seems likely that this difference is due to specific targeting of the Tmab-containing complexes to the overexpressed Her2 receptors which are much more plentiful in the Her18 cells than in the MCF7 cells (16).

In the absence of LLO, there was effectively no luciferase activity in either cell line treated with Tmab/Luc complexes (Figure 6). We have previously shown that LLO is essential for the formation of pores in the endosomal membrane and subsequent transit of calcein payload to the cytoplasm when Tmab-containing liposomes are bound to Her2 receptors and taken up into endosomes (14). Likewise, our results with the Tmab/Luc complexes in the absence of LLO suggest that there is a lack of luciferase activity in either cell line because the Luc-DNA is also unable to cross the endosomal membrane into the cytoplasm of the targeted cells.



### Viability of Her18 cells treated with Tmab/Luc nanocomplexes and luciferase expression over a 3-day time course

To determine if treatment with Tmab/Luc complexes was toxic or non-toxic to Her2-overexpressing breast cancer cells, we simultaneously measured luciferase activity and cell viability of complex-treated versus control non-treated Her18 cells over a 72-hour time period. When examined visually under the microscope, treated and non-treated cells appeared to be identical over time with respect to morphology, viability, and confluency with approximately 40-50% confluency at 24 hours, 75% confluency at 48 hours, and finally complete confluency by 72 hours after treatment.

The apparent lack of effect of nanocomplex treatment on cell viability over 72 hours was confirmed by an XTT viability assay (Figure 7, upper panel). Over the same time period, the complex-treated cells showed a marked increase in luciferase expression (Figure 7, lower panel), suggesting that the cells were viable and continued to synthesize luciferase. As expected, the control Her18 cells, which received only a medium change and no complex treatment, had luciferase readings at the level of background, and are therefore not visualized in the bar graph.

### Targeting Tmab/Luc nanocomplexes to other breast cancer cell lines and competition with free Tmab

To examine the targeting of the Tmab/Luc nanocomplexes to Her2-overexpressing breast cancer cell lines other than MCF7 and MCF7/Her18, we treated ce2 cells and HCC1954 cells with Tmab/Luc nanocomplexes and measured the luciferase expression in the absence versus the presence of free Tmab as competitor. An increase in luciferase expression was noted in both the ce2 and HCC1954 cell lines, in comparison to the low Her2-expressor MCF7 cell line (Figure 8), although both cell lines exhibited less luciferase end product than did the Her18 cells. It is noteworthy that the HCC1954 cell line is trastuzumab-resistant (20) but, in spite of this, specific gene therapy was accomplished with our targeting system. Competition with free Tmab was most effective with the Her18 and HCC1954 cells, less effective with the ce2 cells, and with no competition of the basal luciferase expression in the MCF7 cells (Figure 8).

## Discussion

Overexpression of specific receptors in the plasma membranes of various cancer cells provides a mechanism by which such cells can be targeted specifically *in vitro* and *in vivo* with antibody-containing nanocomplexes. In the case of human breast cancers, overexpression of the human epidermal growth factor receptor 2 (Her2) occurs in 25 – 30% of breast cancers and is associated with an aggressive phenotype (21,22). By conjugating trastuzumab (Herceptin®), an antibody specific for the Her2 receptor, to our DNA-containing complexes, we have achieved specific delivery of DNA to Her2-overexpressing breast cancer cells. In the presence of competitor free Tmab, expression of end product in these cells is markedly decreased, demonstrating that targeted gene expression is indeed dependent on nanocomplexes binding to the Her2 receptors on the cancer cells.

To better conceptualize our DNA-targeting nanocomplex, we provide an interpretive illustration of a single complex (Figure 9). The targeting complexes in our model are based on a core of OPSS-PEG-NHS (OPN), a PEG derivative capable of forming covalent amide linkages at its NHS-end with amino groups of proteins and disulfide bonds at its OPSS-end with thiol groups in proteins. After binding of polylysine (PL) to the NHS-ends of OPN, supercoiled plasmid DNA is added and interacts with the bound PL via noncovalent electrostatic interactions. Finally thiolated trastuzumab (t-Tmab) and LLO compete for the OPSS-ends of OPN to form reversible disulfide bonds. The electrostatic bonds are responsible for the subsequent release of DNA and the reversible disulfide bonds for the release of LLO from the complex within the interior of the endosomes (14, 24).

The addition of the pore-forming protein, LLO, to our nanocomplexes enables the successful transit of the DNA from the endosomal compartments to the cytoplasm of the targeted cells. Under the reducing conditions found in endosomes, disulfide-bound LLO is released either from low molecular weight PEIs (24) or from liposomes (2,14,25) such that it can form pores in the endosomal membrane and allow exit of the delivered endosomal contents to the cytoplasm. We have now extended these findings by showing that the disulfide bond between the LLO and the OPN core in our nanocomplexes also appears to be reduced in the endosome, and the released LLO then functions to allow passage of the DNA to the cytoplasm. In addition, the acidic environment of the endosome presumably affects the ionic bonds between the DNA and the PL, resulting in dissociation of the DNA from the polylysine, while the PL itself would remain covalently bonded to the OPN core.

It is assumed that the DNA in our system is expressed only in targeted cells that are actively dividing because, once delivered to the cytoplasm, DNA molecules must relocate to the nucleus, during breakdown and reformation of the nuclear membrane, in order for transcription to take place (26). The transcripts subsequently exit the nucleus and are translated in the cytoplasm to result in detectable gene product. In our studies, we have successfully detected two different gene products, green fluorescent protein and luciferase, as a result of specific delivery of their respective DNAs to Her2 overexpressing cells by our Tmab-coupled nanocomplexes. Expression of GFP and luciferase in our system is dependent on the presence of both Tmab and LLO in the DNA-containing targeting complexes. Omission of either in construction of the nanocomplexes results in a marked decrease in expression of these gene products in cells grown *in vitro*.

The DNA-containing nanocomplexes that we have designed could be constructed using any plasmid DNA coding for a desired gene product, such as IL-12 which can stimulate a T-cell response or TNF-alpha which can induce apoptosis in tumor cells. Non-specific delivery of these therapeutic genes results in significant toxicity, necessitating a system that results in tumor-specific gene delivery (27-29). In addition to versatility of gene delivery, it should be straightforward to substitute Tmab with any other desired antibody or targeting peptide that binds to receptors uniquely overexpressed on the cells being targeted. Our complexes are stable to storage for a period of more than 6 weeks at 4°C without loss of activity (data not shown), both with respect to targeting ability and expression of luciferase. Finally, our toxicity experiments show that our nanocomplexes are not toxic to Her18 cells for at least 72

hours after Tmab-targeting and in fact allow subsequent growth of Her2-overexpressing cells *in vitro*.

The specificity and other desirable characteristics demonstrated for our gene delivery system *in vitro* justify further study in an *in vivo* model. It must be determined whether our nanocomplexes are capable of reaching their intended target *in vivo* before being degraded or cleared from the circulatory system and whether LLO or any other component present in our targeting complexes is sequestered sufficiently so as not to trigger an immune response in recipient tumor-bearing animals.

## Acknowledgments

We thank Dr. Richard Kullberg for critical reading of the manuscript and help in preparing the graphics, as well as many helpful discussions on our targeting system. This work was supported by the WWAMI Medical Education Program, University of Alaska Anchorage, Alaska Run for Women Grants to K.M. and M.K., and an Institutional Development Award (IDeA) from the National Institutes of Health/National Institute of General Medical Sciences under grant #P20GM103395 to M.K.

## References

1. Hayes ME, Drummond DC, Hong K, Zheng WW, Khorosheva VA, Cohen JA, Noble CO, et al. Increased target specificity of anti-HER2 genospheres by modification of surface charge and degree of PEGylation. *Mol Pharmaceut*. 2006; 3:726–736.
2. Kullberg M, McCarthy R, Anchordoquy TJ. Gene delivery to Her-2+ breast cancer cells using a two-component delivery system to achieve specificity. *Nanomedicine*. 2014; 10:1253–1262. [PubMed: 24632244]
3. Tagalakis AD, Grosse SM, Meng QH, Mustapa MFM, Kwok A, Salehi SE, et al. Integrin-targeted nanocomplexes for tumour specific delivery and therapy by systemic administration. *Biomaterials*. 2011; 32:1370–1376. [PubMed: 21074847]
4. Ikegami S, Yamakami K, Ono T, Sato M, Suzuki S, Yoshimura I, et al. Targeting gene therapy for prostate cancer cells by liposomes complexed with anti-prostate-specific membrane antigen monoclonal antibody. *Human Gene Ther*. 2006; 17:997–1005. [PubMed: 17032155]
5. Wolschek MF, Thallinger C, Kursa M, Rossler V, Allen M, Lichtenberger C, et al. Specific systemic nonviral gene delivery to human hepatocellular carcinoma xenografts in SCID mice. *Hepatology*. 2002; 36:1106–1114. [PubMed: 12395320]
6. Chiu SJ, Ueno NT, Lee RJ. Tumor-targeted gene delivery via anti-HER2 antibody (trastuzumab, Herceptin®) conjugated polyethylenimine. *J Control Release*. 2004; 97:357–369. [PubMed: 15196762]
7. Kircheis R, Ostermann E, Wolschek MF, Lichtenberger C, Magin-Lachmann C, Wightman L, et al. Tumor-targeted gene delivery of tumor necrosis factor- $\alpha$  induces tumor necrosis and tumor regression without systemic toxicity. *Cancer Gene Ther*. 2002; 9:673–680. [PubMed: 12136428]
8. Koppu S, Oh YJ, Edrada-Ebel R, Blatchford DR, Tetley L, Tate RJ, et al. Tumor regression after systemic administration of a novel tumor-targeted gene delivery system carrying a therapeutic plasmid DNA. *J Control Release*. 2010; 143:215–221. [PubMed: 19944722]
9. Li D, Ping Y, Xu F, Yu H, Pan H, Huang H, et al. Construction of a star-shaped copolymer as a vector for FGF receptor-mediated gene delivery *in vitro* and *in vivo*. *Biomacromolecules*. 2010; 11:2221–2229. [PubMed: 20704346]
10. Lim LY, Koh PY, Somani S, Robaian MA, Karim R, Yean YL, et al. Tumor regression following intravenous administration of lactoferrin- and lactoferricin-bearing dendriplexes. *Nanomedicine: Nanotechnology, Biology, and Medicine*. 2015; 11:1445–1454.
11. Moghimi SM, Symonds P, Murray JC, Hunter AC, Debska G, Szewczyk A. A two-stage poly(ethyleneimine)-mediated cytotoxicity: implications for gene transfer/therapy. *Mol Ther*. 2005; 11:990–995. [PubMed: 15922971]

12. Kircheis R, Wightman L, Kursa M, Ostermann E, Wagner E. Tumor-targeted gene delivery: an attractive strategy to use highly active effector molecules in cancer treatment. *Gene Ther.* 2002; 9:731–735. [PubMed: 12032698]
13. Glomski JJ, Gedde MM, Tsang AW, Swanson JA, Portnoy DA. The *Listeria monocytogenes* hemolysin has an acidic pH optimum to compartmentalize activity and prevent damage to infected host cells. *J Cell Biol.* 2002; 156:1029–1038. [PubMed: 11901168]
14. Kullberg M, Owens JL, Mann K. Listeriolysin O enhances cytoplasmic delivery by Her-2 targeting liposomes. *J Drug Target.* 2010; 18:313–320. [PubMed: 20201742]
15. D'Souza B, Berdichevsky F, Kyprianou N, Taylor-Papadimitriou J. Collagen-induced morphogenesis and expression of the alpha 2-integrin subunit is inhibited in c-erbB2-transfected human mammary epithelial cells. *Oncogene.* 1993; 8:1797–1806. [PubMed: 8099725]
16. Benz CC, Scott GK, Sarup JC, Johnson RM, Tripathy D, Coronado E, et al. Estrogen dependent, tamoxifen-resistant tumorigenic growth of MCF-7 cells transfected with HER2/neu. *Breast Cancer Res Treat.* 1992; 24(2):85–95. [PubMed: 8095168]
17. Lee KD, Oh YK, Portnoy DA, Swanson JA. Delivery of macromolecules into cytosol using liposomes containing hemolysin from *Listeria monocytogenes*. *J Biol Chem.* 1996; 271:7249–7252. [PubMed: 8631734]
18. Schnupf P, Portnoy DA. Listeriolysin O: a phagosome-specific lysin. *Microbes Infect.* 2007; 9:1176–1187. [PubMed: 17720603]
19. Kullberg M, Mann K, Owens JL. A two-component drug delivery system using Her-2-targeting thermosensitive liposomes. *J Drug Targeting.* 2009; 17:98–107.
20. Sahin O, Frohlich H, Lobke C, Korf U, Burmester S, Majety M, et al. Modeling ERBB receptor-regulated G1/S transition to find novel targets for *de novo* trastuzumab resistance. *BMC Systems Biology.* 2009; 3:1. E-pub ahead of print. doi: 10.1186/1752-0509-3-1 [PubMed: 19118495]
21. Azambuja E, Durbecq V, Rosa DD, Colozza M, Larsimont D, Piccart-Gebhart M, et al. HER-2 overexpression/amplification and its interaction with taxane-based therapy in breast cancer. *Ann Oncol.* 2008; 19:223–232. [PubMed: 17872901]
22. Engel RH, Kaklamani VG. HER2-positive breast cancer: current and future treatment strategies. *Drugs.* 2007; 67:1329–1341. [PubMed: 17547474]
23. Pai SS, Hammouda B, Hong K, Pozzo DC, Przybycien TM, Tilton RD. The conformation of the poly(ethylene glycol) chain in mono-PEGylated lysozyme and mono-PEGylated human growth hormone. *Bioconjugate Chem.* 2011; 22:2317–2323.
24. Choi S, Lee KD. Enhanced gene delivery using disulfide-crosslinked low molecular weight polyethylenimine with listeriolysin o-polyethylenimine disulfide conjugate. *J Control Release.* 2008; 131:70–76. [PubMed: 18692533]
25. Kullberg M, Mann K, Anchordoquy TJ. Targeting Her-2+ breast cancer cells with bleomycin immunoliposomes linked to LLO. *Mol Pharmaceut.* 2012; 9(7):2000–2008. E-pub ahead of print 4 Jun 2012. DOI: 10.1021/mp300049n
26. Duan Y, Zhang S, Wang B, Yang B, Zhi D. The biological routes of gene delivery mediated by lipid-based non-viral vectors. *Expert Opin Drug Deliv.* 2009; 6:1351–1361. [PubMed: 19780710]
27. Marr RA, Hitt M, Muller WJ, Gaudie J, Graham FL. Tumour therapy in mice using adenovirus vectors expressing human TNFalpha. *Int J Oncol.* 1998; 12:509–515. [PubMed: 9472086]
28. Salem ML, Gillanders WE, Kadima AN, El-Naggar S, Rubinstein MP, Demcheva M, et al. Review: novel nonviral delivery approaches for interleukin-12 protein and gene systems: curbing toxicity and enhancing adjuvant activity. *J Interferon Cytokine Res.* 2006; 26:593–608. [PubMed: 16978064]
29. Yerbes R, Palacios C, Lopez-Rivas A. The therapeutic potential of TRAIL receptor signalling in cancer cells. *Clin Transl Oncol.* 2011; 13:839–847. [PubMed: 22126726]

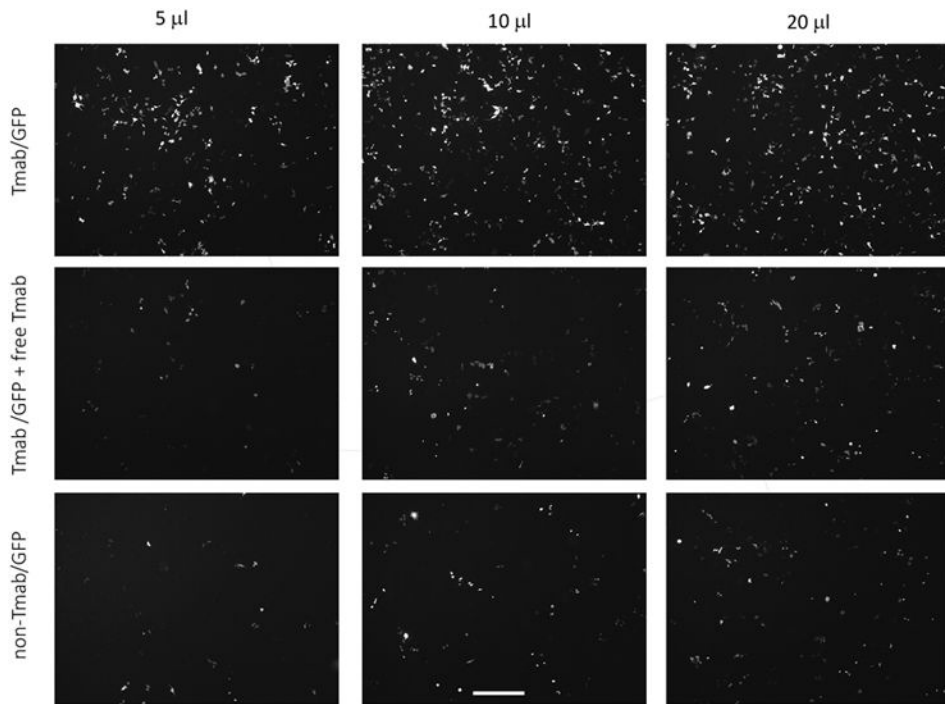


**Figure 1.**

GFP expression in ce2 cells treated with GFP-nanocomplexes. Ce2 cells were treated for 3 hrs with GFP DNA complexes (dosages from 5  $\mu$ l to 20  $\mu$ l) containing LLO and Tmab (upper row), containing LLO and Tmab along with free Tmab in the medium as competitor (middle row), or containing LLO without Tmab in the complexes (lower row). Fluorescent cells were visualized 48 hrs after treatment with an inverted fluorescence microscope, and photographs taken with the 5 $\times$  objective. The scale bar equals 500 microns.

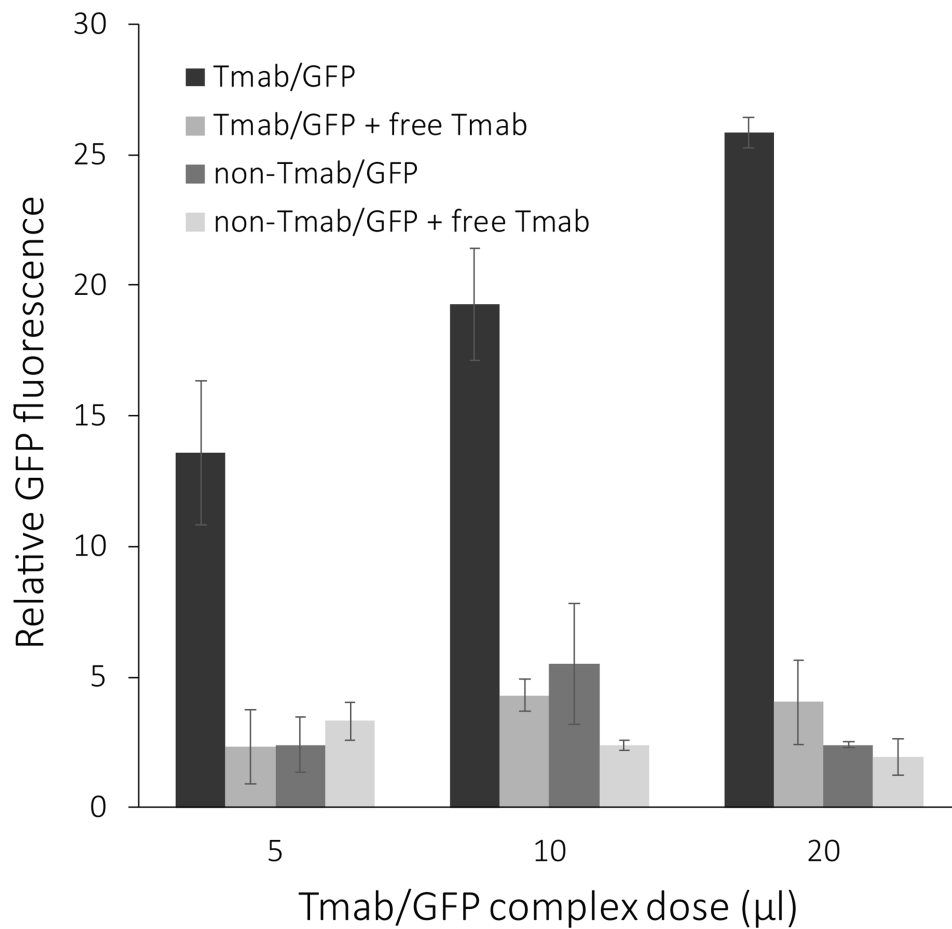


**Figure 2.**

Effect of Tmab on GFP expression. Bars represent the data analysis of the relative GFP fluorescence in ce2 cells such as shown in Figure 1. The cells were treated for 3 hrs with 5  $\mu$ l to 20  $\mu$ l doses of GFP complexes either containing Tmab (black bar) or not containing Tmab (dark grey bar). The effect of competition with free Tmab (2.5  $\mu$ l/well) is shown at each dosage. Fluorescent cells were visualized 48 hrs after treatment with an inverted fluorescence microscope, and photographs were taken with the 5 $\times$  objective. Quantification of the fluorescence in each field was done with NIH ImageJ, and the data were plotted as the mean  $\pm$  S.E. (n = 4 for treatment with Tmab complex, and n = 2 for all other treatments).



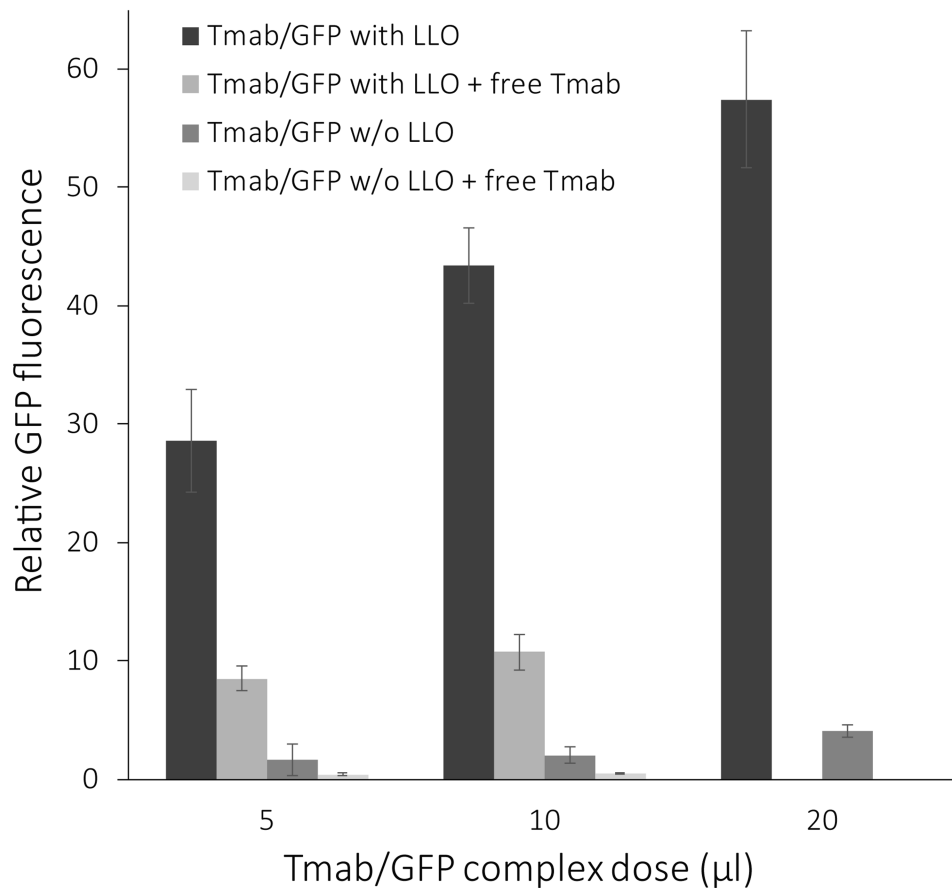


**Figure 3.**

Effect of LLO on GFP expression. Bars indicate the relative fluorescence of GFP in ce2 cells treated with Tmab/GFP complexes with and without LLO and competed with free Tmab. Cells were treated with Tmab/GFP complexes (dosages from 5  $\mu$ l to 20  $\mu$ l) containing LLO (black bar) or not containing LLO (dark grey bar). To test the effect of competition on GFP expression, ce2 cells were treated with complexes in the presence of free Tmab (2.5  $\mu$ l/well) for the 5  $\mu$ l and 10  $\mu$ l doses of GFP-complexes but not for the 20  $\mu$ l dose. Fluorescent cells were visualized 48 hrs after treatment with an inverted fluorescence microscope, and photographs were taken with the 5 $\times$  objective. Quantification of the fluorescence in each field was done with NIH ImageJ, and the data are shown as the mean  $\pm$  S.E. (n = 2).

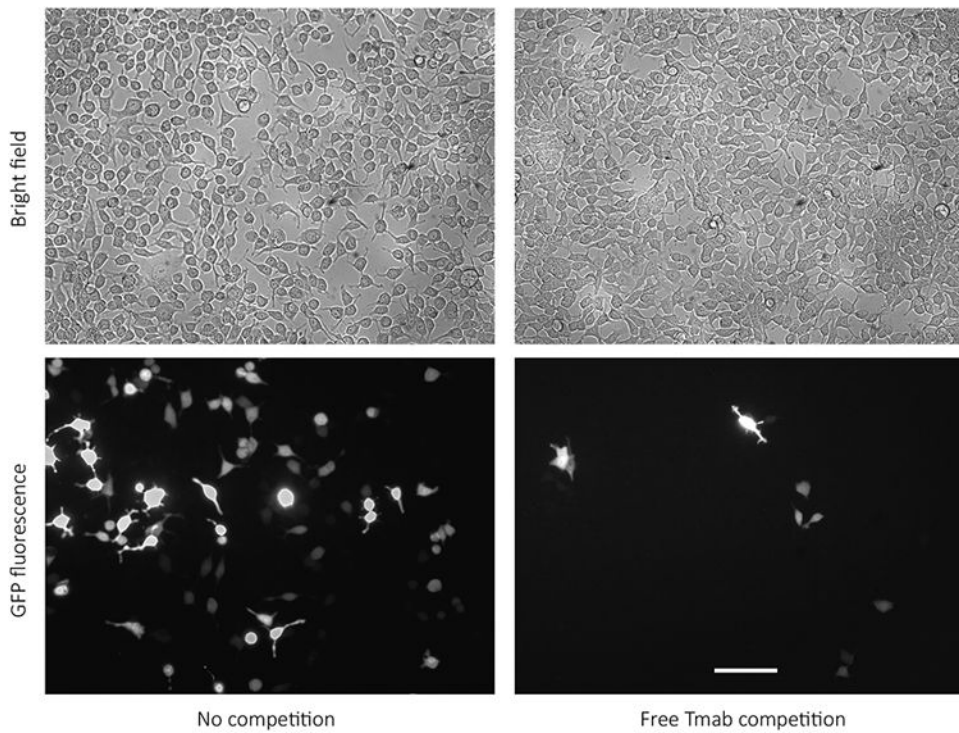


**Figure 4.**

Fluorescence in Her18 cells treated with Tmab/GFP complexes. Her18 cells were treated for 3 hrs with a 10  $\mu\text{l}$ /well dose of Tmab/GFP complexes either in the absence or in the presence of free Tmab competitor (2.5  $\mu\text{l}$ /well) and visualized 48 hrs later. A bright field image and a fluorescent image of the same field were taken for comparison, with the 20 $\times$  objective on the inverted fluorescence microscope. The scale bar equals 100 microns.

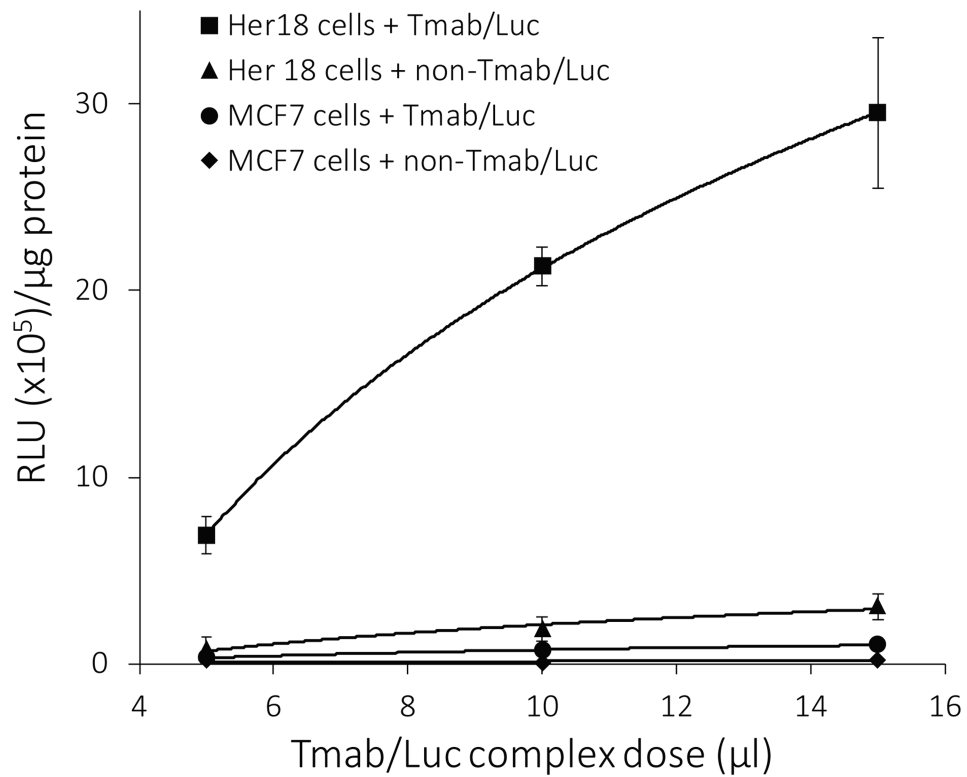


**Figure 5.**

Effect of Tmab on luciferase activity. Luciferase activity ( $\text{RLU} \times 10^5$  units/ $\mu\text{g}$  protein) is plotted against dose (5  $\mu\text{l}$  to 15  $\mu\text{l}$ ) of DNA complexes used for treatment. Data are compared for Her18 versus MCF7 cells targeted with Luc-complexes containing LLO and with or without Tmab present in the complexes. Each treatment was set up in triplicate, and cells were harvested 24 hours after treatment for analysis of luciferase activity. BCA protein determinations were done on the same cell extracts used for the luciferase assay. The data are shown as the mean  $\pm$  S.E. ( $n = 3$ ).

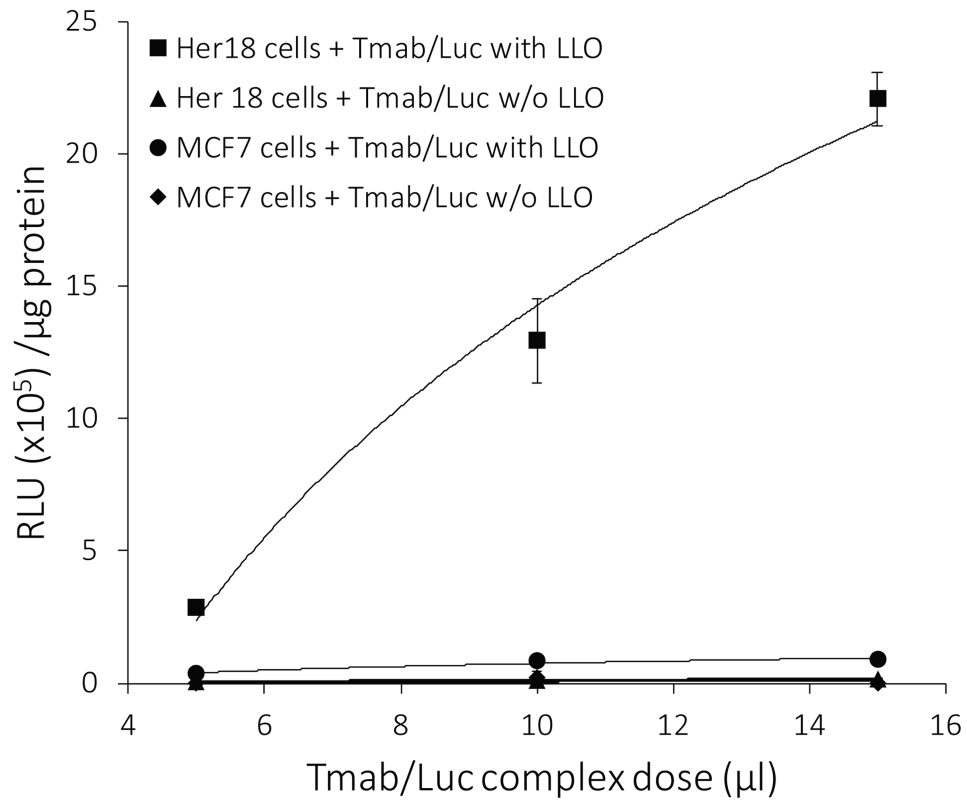


**Figure 6.**

Effect of LLO on luciferase activity. Luciferase activity ( $\text{RLU} \times 10^5 \text{ units}/\mu\text{g protein}$ ) expressed in Her18 versus MCF7 cells is plotted against dose ( $5 \mu\text{l}$  to  $15 \mu\text{l}$ ) of DNA complexes used for treatment. Cells were treated with DNA complexes containing Tmab/Luc and with or without LLO. Each treatment was set up in triplicate, and cells were harvested 24 hours after treatment for analysis of luciferase activity. BCA protein determinations were done on the same cell extracts used for the luciferase assay. The data are shown as the mean  $\pm$  S.E. ( $n = 3$ ).

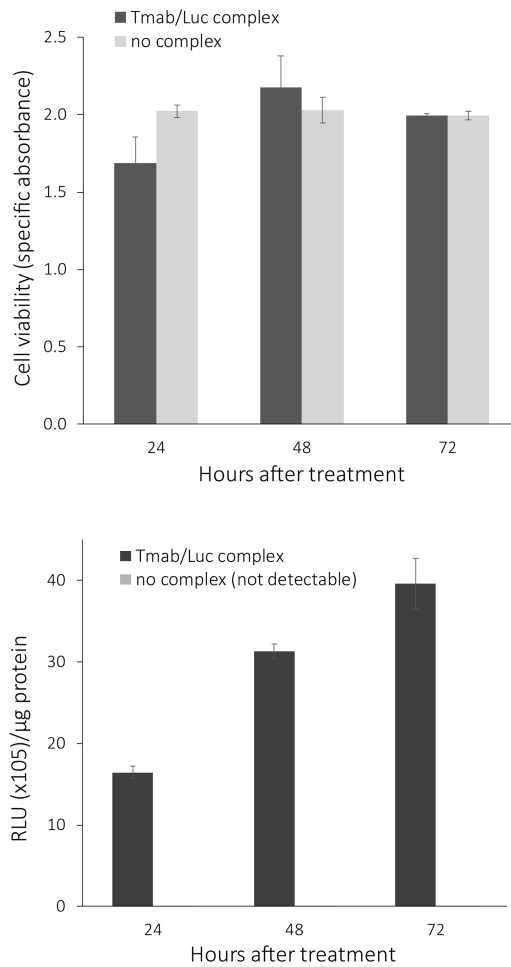


**Figure 7.**

Effect of Tmab/Luc complex treatment on cell viability. Charts show XTT viability (upper panel) and luciferase activity (RLU  $\times 10^5$  units/ $\mu\text{g}$  protein, lower panel) of Her18 cells at 24 hr, 48 hr, and 72 hr after an initial 3-hour treatment with 90  $\mu\text{l}$  medium plus 10  $\mu\text{l}$ /well of Tmab/Luc complex or with 100  $\mu\text{l}$  medium/well as a control (no complex). BCA protein determinations were done on the same cell extracts used for the luciferase assay. The control cells without any complexes had no detectable luciferase activity above the baseline. The data are shown as the mean  $\pm$  S.E. (n = 3).

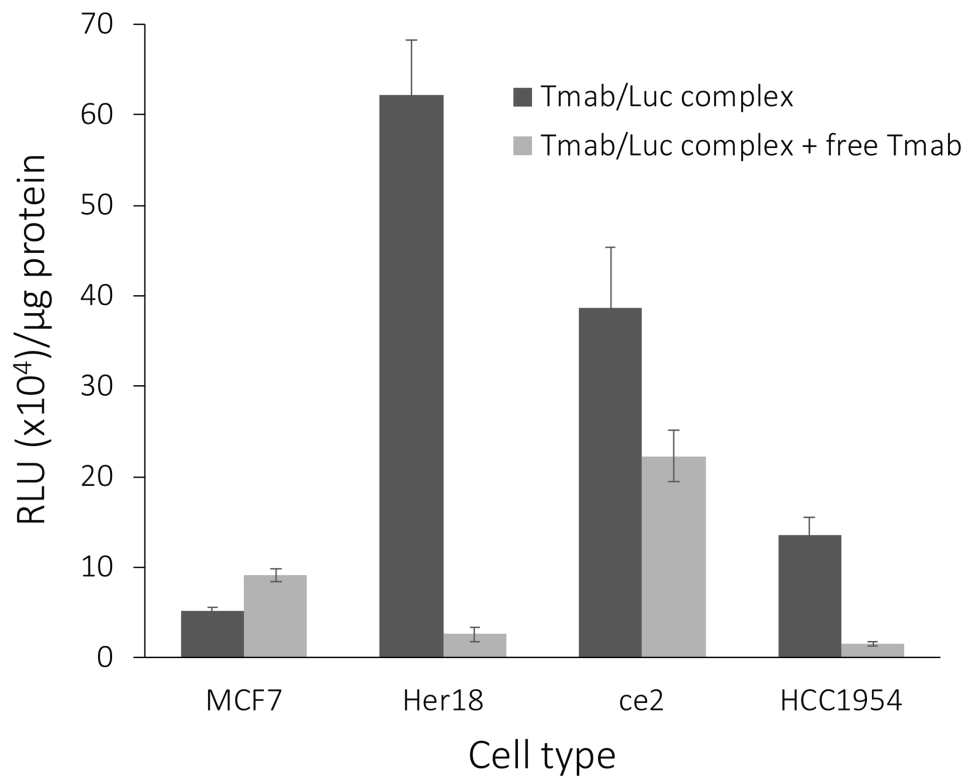


**Figure 8.**

Expression of luciferase in 4 cancer cell lines and competition with free Tmab. Cell lines MCF7, Her18, ce2, and HCC1954 grown in 96-well plates were treated with 10  $\mu$ l/well of Tmab/Luc complexes for 3 hrs without or with free Tmab competitor (2.5  $\mu$ l/well) present. Cells were harvested 24 hours after treatment for analysis of luciferase activity (RLU  $\times$  10<sup>4</sup> units/ $\mu$ g protein). The data are shown as the mean  $\pm$  S.E. (n = 3).



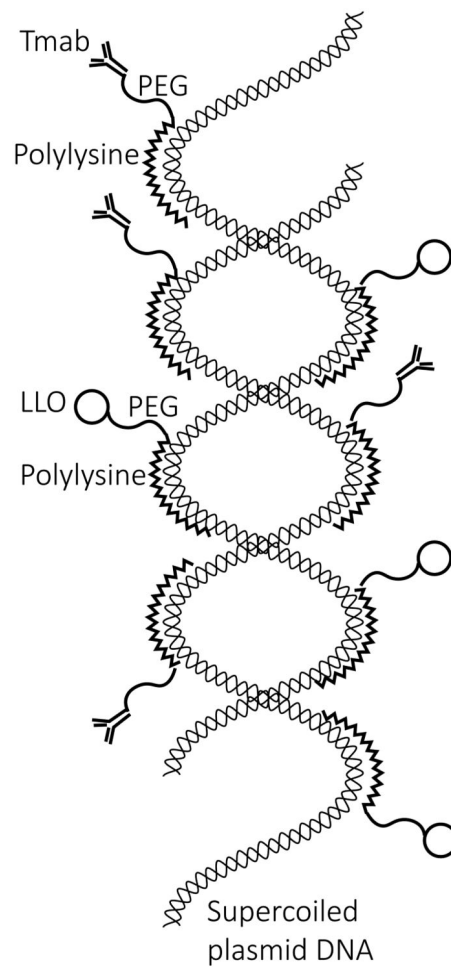


**Figure 9.**

Illustration of a single Tmab-targeted DNA nanocomplex. A supercoiled double-helical plasmid DNA molecule is shown in the interior, decorated with numerous Tmab-PEG-PL molecules and LLO-PEG-PL molecules on the exterior. The PEG found in each of these attachments is envisioned as a flexible arm protruding out from the PL bound to the supercoiled DNA molecule. Small-angle neutron scattering studies of mono-PEGylated conjugates, in which PEG is covalently linked to a protein, assume a dumbbell configuration rather than a shroud configuration (23). Presumably this would leave the Tmab positioned in such a way as to be able to bind to the Her2 receptors in the plasma membranes of targeted cells.

The molecular weights of the individual components in the nanocomplex are as follows: plasmid DNA = 4.7 kb (pEGFP-N3) or 5.9 kb (NanoLuc), Tmab = 145.5 kDa, LLO = 58 kDa, PL = 37 kDa, and PEG = 5 kDa. The overall size of the nanocomplex is 150–250 nm.